RESEARCH ARTICLE

Kinematics of Ribbon-Fin Locomotion in the Bowfin, *Amia calva*

JOURNAL OF EXPERIMENTAL ZOOLOGY
PART A
ECOLOGICAL GENETICS AND PHYSIOLOGY
A Journal of Integrative Biology

KEVIN JAGNANDAN[1,2]* AND CHRISTOPHER P. SANFORD[1]

[1]Department of Biology, Hofstra University, Hempstead, New York
[2]Department of Evolution, Ecology and Organismal Biology, University of California, Riverside, California

ABSTRACT

An elongated dorsal and/or anal ribbon-fin to produce forward and backward propulsion has independently evolved in several groups of fishes. In these fishes, fin ray movements along the fin generate a series of waves that drive propulsion. There are no published data on the use of the dorsal ribbon-fin in the basal freshwater bowfin, *Amia calva*. In this study, frequency, amplitude, wavelength, and wave speed along the fin were measured in *Amia* swimming at different speeds (up to 1.0 body length/sec) to understand how the ribbon-fin generates propulsion. These wave properties were analyzed to (1) determine whether regional specialization occurs along the ribbon-fin, and (2) to reveal how the undulatory waves are used to control swimming speed. Wave properties were also compared between swimming with sole use of the ribbon-fin, and swimming with simultaneous use of the ribbon and pectoral fins. Statistical analysis of ribbon-fin kinematics revealed no differences in kinematic patterns along the ribbon-fin, and that forward propulsive speed in *Amia* is controlled by the frequency of the wave in the ribbon-fin, irrespective of the contribution of the pectoral fin. This study is the first kinematic analysis of the ribbon-fin in a basal fish and the model species for Amiiform locomotion, providing a basis for understanding ribbon-fin locomotion among a broad range of teleosts. *J. Exp. Zool. 319A:569–583, 2013.*

J. Exp. Zool. 319A:569–583, 2013

How to cite this article: Jagnandan K, Sanford CP. 2013. Kinematics of ribbon-fin locomotion in the bowfin, *Amia calva*. J. Exp. Zool. 319A:569–583.

There are over 25,000 species of ray-finned fishes with a tremendous diversity in body form and numerous adaptations for locomotion. Methods of aquatic locomotion are generally classified as body and/or caudal fin (BCF) locomotion, or median and/or paired fin (MPF) locomotion (Breder, '26; Lindsey, '78; Webb and Blake, '85). As the name implies, BCF swimmers rely primarily on axial body and caudal fin movements to produce thrust, while MPF swimmers utilize the dorsal, anal, and/or pectoral fins for propulsion. As a model of MPF swimmers, two swimming modes involve the use of a single undulatory median fin for propulsion, Amiiform locomotion and Gymnotiform locomotion. These forms of swimming, collectively termed ribbon-fin locomotion, involve undulating an elongated dorsal fin (Amiiform) and/or anal fin (Gymnotiform) to produce a series of waves that propel the organism forwards or backwards. Interestingly, ribbon-fin locomotion has independently evolved in a variety of marine and freshwater teleost fishes. This is demonstrated (a) dorsally in the bowfin (*Amia calva*) (Amiiformes), African aba aba (*Gymnarchus niloticus*) (Osteoglossiformes: Gymnarchidae), and oarfish (Lampriformes: Regalecidae); (b) ventrally in ghost knifefish (Gymnotiformes) and notopterid knifefishes (Osteoglossiformes: Notopteridae); and (c) both

Grant sponsor: National Science Foundation; grant numbers: IOS 0444891, DBI 0420440, DBI 0963167, DBI 1126234; grant sponsor: Department of Biology at Hofstra University.
*Correspondence to: Kevin Jagnandan, Department of Evolution, Ecology and Organismal Biology, University of California, 3401 Watkins Drive UC Riverside, Room 1229, Spieth Hall, Riverside, CA 92521.
E-mail: kevin.jagnandan@email.ucr.edu
Received 14 May 2013; Revised 30 July 2013; Accepted 31 July 2013
DOI: 10.1002/jez.1819
Published online 3 September 2013 in Wiley Online Library (wileyonlinelibrary.com).

dorsally and ventrally in seahorses and pipefishes (Syngnathiformes: Syngnathidae), triggerfishes (Tetraodontiformes: Balistidae), filefishes (Tetraodontiformes: Monacanthidae), and some eels (Anguilliformes: Protanguillidae; Fig. 1).

Research on ribbon-fin use across these evolutionarily distinct groups is limited. Previous studies have suggested ribbon-fin locomotion was an adaptation for slow swimming with high mechanical and hydrodynamic efficiency (Blake, '83). Others have analyzed the hydrodynamics of ribbon-fin swimming with an emphasis on its role in weakly electric fish (e.g., ghost knifefish) (Shirgaonkar et al., 2008; MacIver et al., 2010). These studies suggest that ribbon-fin locomotion provides increased maneuverability and allows the fish to hold its body rigid while swimming. This reduces modulations of the electric field generated from the body of the fish, thus maximizing electrosensory reception for prey capture, communication, and detecting environmental cues. Additional studies on ribbon-fin locomotion have focused on the development of biomimetic robotic models

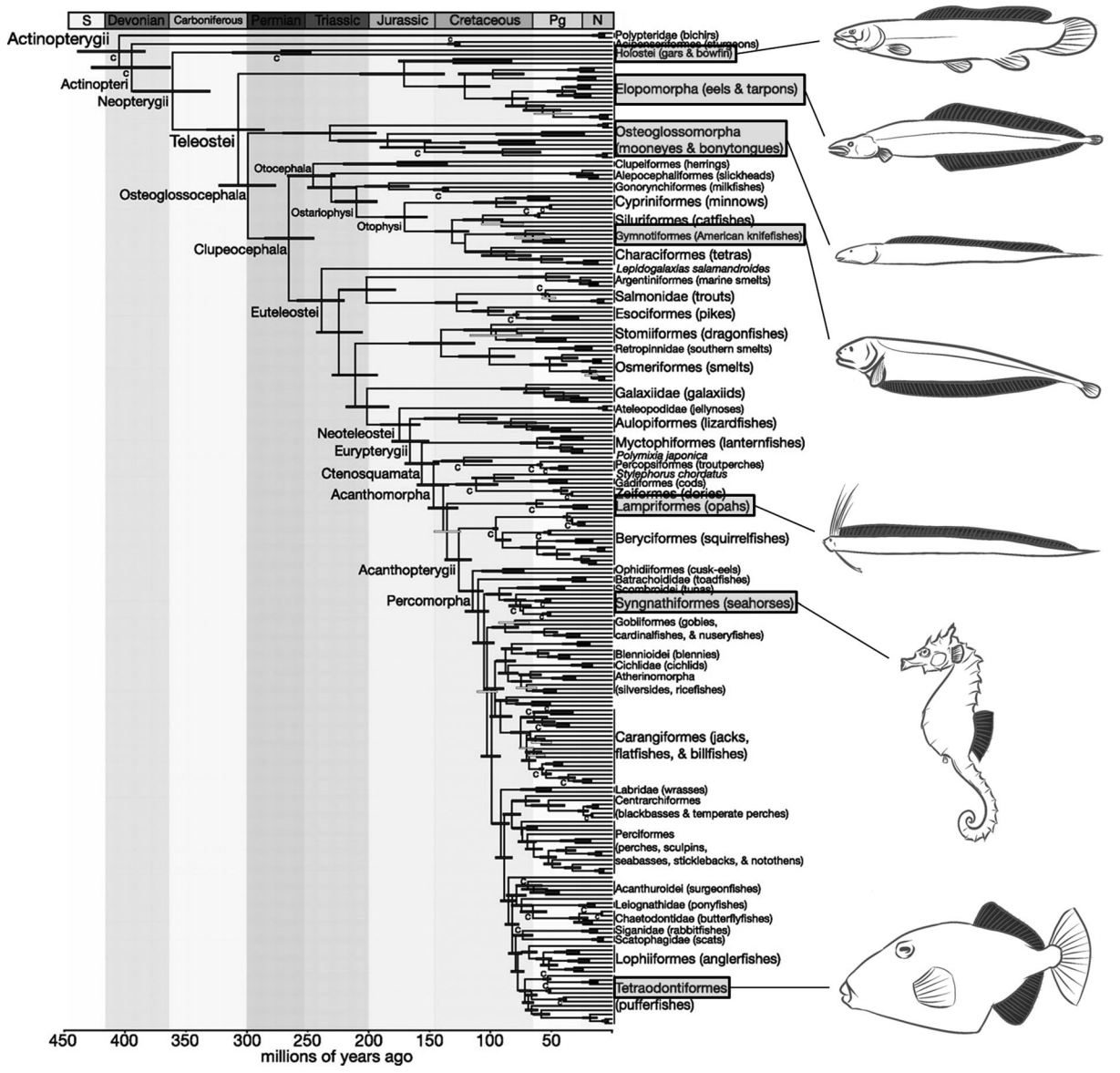

Figure 1. Phylogeny of fishes highlighting the convergent evolution of ribbon-fin locomotion. Highlighted taxa contain species equipped with an elongated dorsal and/or anal fin (shaded) used for ribbon-fin swimming. This phylogeny is not inclusive of all representatives of ribbon-fin locomotion. Images are not to scale (reproduced and modified from Near et al., 2012).

based on the structural design and efficiency of this mode of locomotion (MacIver et al., 2004; Epstein et al., 2006; Hu et al., 2009; Zhou et al., 2010; Curet et al., 2011).

It is notable that very few studies have addressed the movements of the ribbon-fin during propulsion. Although the kinematics of undulatory waves along elongated dorsal and anal fins were briefly described in seahorses (Blake, '76, '80), in some gymnotids and notopterids (Blake, '83; Shirgaonkar et al., 2008; Ruiz-Torres et al., 2012), and in the African aba aba (*Gymnarchus niloticus*) (Fei et al., 2005), there are several assumptions associated with these studies that make it difficult to infer how the ribbon-fin controls swimming speed or to directly compare ribbon-fin propulsion among species. In addition to small sample size (generally one individual), there are several assumptions regarding ribbon-fin use as a propulsive mechanism. First, the location at which measurements of wave parameters were taken along the fin is not described, thus assuming the wave pattern is the same along the length of the ribbon-fin. Furthermore, previous studies do not address the possibility of other fins contributing to propulsion during ribbon-fin locomotion.

This study aims to address these assumptions while investigating the kinematics of ribbon-fin locomotion in a basal fish species, often identified as the model of Amiiform swimming. The bowfin is a primitive actinopterygian fish whose common name originates from its elongated "bow-shaped" dorsal ribbon-fin that runs approximately two-thirds the length of the body. Unlike other Amiiform species with a much longer dorsal ribbon-fin that tapers to a point at the tail, the dorsal fin of *Amia* terminates at the caudal peduncle just anterior of a distinct isocercal caudal fin (Grande and Bemis, '98), which is utilized for swimming at faster speeds and burst swimming. Bowfin are found throughout North America in slow-moving freshwater streams, lakes, and swamps, and rely on the use of the ribbon-fin for sustained swimming and to slowly stalk unsuspecting prey (e.g., small fish, crustaceans, and worms) with minimal disturbance in the water column before a strike. Bowfin were chosen for study because of their position near the base of the ray-finned fish phylogeny (Hurley et al., 2007). As the most basal ribbon-fin swimmer, data on swimming in bowfin will provide valuable baseline data for evolutionary comparisons of ribbon-fin convergence.

Specifically, we addressed three questions in regards to ribbon-fin locomotion in *Amia*. (1) Do the wave properties of the ribbon-fin differ along the length of the fin? Because previous studies did not identify how or where wave parameters were measured along the fin, we aimed to quantify ribbon-fin movements at anterior and posterior regions of the fin to determine if any regional differences occur. (2) How is the ribbon-fin used to control swimming speed? Wave properties of the ribbon-fin are used to establish the primary mechanism for changing speed. (3) Is the ribbon-fin the primary propulsor at slow swimming speeds? Preliminary analyses suggest the potential for pectoral fin use in generating propulsion in addition to simultaneous ribbon-fin undulations. Because the use of the pectoral fins during ribbon-fin locomotion is undocumented in the literature, we aimed to determine if pectoral fin movements are contributing to swimming speed, or if they are serving another role (e.g., producing lift). To do so, we compared ribbon-fin movements with and without the contribution of the pectoral fins, as well as the relationship between pectoral fin movements and swimming speed.

MATERIALS AND METHODS

Animals

Live bowfin (*Amia calva*) were obtained from commercial vendors in Long Island, NY and Florida, and housed individually in 75.7-L (76.2 cm × 30.5 cm × 30.5 cm) and 208.2-L (121.9 cm × 33.0 cm × 53.3 cm) rectangular aquariums in the Hofstra University Animal Laboratory. Stock tanks were maintained at a temperature of 19 ± 1°C. Bowfin (n = 4) ranged in size from 28.7 −33.2 cm (mean ± SEM = 30.1 ± 2.1 cm) with a ribbon-fin length (RFL; measured at the base of the fin) of 12.7–15.5 cm (mean ± SEM = 13.6 ± 1.3 cm), and a ribbon-fin area (RFA) of 18.4–26.5 cm^2 (mean ± SEM = 24.0 ± 3.8 cm^2), measured using ImageJ. Individuals showed no significant damage or deterioration of the dorsal, pectoral, or caudal fins. The fish were fed a mixed diet of live goldfish (*Carassius auratus auratus*) and night crawler earthworms (*Lumbricus terrestris*) approximately three times a week.

Experimental Setup

To examine the movements of the ribbon-fin during slow swimming, individuals were observed swimming in the 80 cm × 25 cm × 25 cm rectangular working section of a 150-L recirculating flume (Loligo Model 150 L, Loligo Systems, Tjele, Denmark) maintained at 19 ± 1°C. A 2.5 mm thick 35 cm × 28 cm

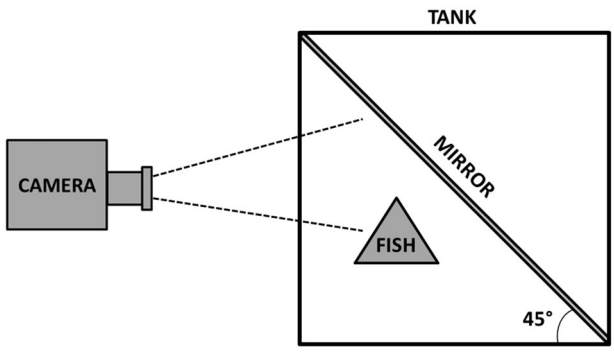

Figure 2. A schematic diagram of the experimental set up in posterior view. One camera was used to record the dorsal view of the ribbon-fin using the mirror. A second camera (not shown) was used to verify movement of the pectoral fins during ribbon-fin swimming (diagram not to scale).

mirror with a tapering leading edge was mounted in the working section at a 45° angle above the fish to provide a dorsal view of the ribbon-fin during steady swimming (Fig. 2). The thin mirror was supported above using plastic honeycomb material and the leading edge was flush with the honeycomb sheet of the working section upstream to avoid leading edge vortices. Planar digital particle image velocimetry (DPIV) at 3 cm increments at several locations revealed that flow was laminar throughout the working section with a boundary layer no thicker than 1.2 cm at all flow speeds used. Additional honeycomb was used to create a barrier that restricted swimming while still providing adequate space for the fish to swim steadily in the center of the water column below the mirror. Separate experiments were conducted to record pectoral fin kinematics, utilizing a camera mounted underneath the working section to obtain a ventral view of the fish ($n = 2$).

Videography

Prior to each experiment, each animal was placed in the experimental arena and acclimated for 45–60 min. Individuals were filmed swimming against varying flow speeds from 0.2 to 1.0 body length per second (BL/sec) at increments of 0.2 BL/sec. These flow speeds were necessary for recording sustained swimming with the use of the ribbon-fin prior to the gait transition to BCF swimming observed at higher speeds during preliminary investigations. Individuals were subjected to increasing, decreasing, and randomized flow speeds for no more than 5 min at a time, and 5–10 min rest periods were provided to avoid trends or patterns associated with fatigue. Rest periods were extended at higher swimming speeds. Videos were only recorded when the fish was swimming in the center of the working section with at least 3 cm clearance from any surface, which was sufficient to avoid boundary layer effects (Tytell and Lauder, 2004; Carlson and Lauder, 2011). Only sequences with no evident changes in pitch, roll, or yaw, and no movement of the body or caudal fin were analyzed. In all of the experiments, animals were recorded swimming under illumination by a 250 W halogen light.

Video for ribbon-fin kinematics were recorded at 40 frames per second (fps) simultaneously by two Dalsa Genie™ HM1400 cameras and StreamPix 5 software (Norpix, Canada). The first camera recorded a dorsal view of the ribbon-fin for kinematic analysis (Fig. 2). The second camera recorded the pectoral fins solely to verify whether the pectoral fins were being used during ribbon-fin swimming. Videos for simultaneous ribbon-fin and pectoral fin use were only included in the analysis if both pectoral fins moved synchronously in a manner that would likely drive propulsion. In separate experiments for detailed kinematics of pectoral fin movements, a single high-speed Photron Fastcam-X 1280 PCI camera recorded a ventral view of the pectoral fins at 125 fps using Photron Motion Tools software. The dorsal fin was visually monitored to ensure that ribbon-fin undulations were occurring simultaneously.

Video Analysis

Video recordings were analyzed using Track Eye Motion Analysis (TEMA) 3.0 (Image Systems AB, Linkoping, Sweden) software to manually track ribbon-fin and pectoral fin movements during sustained swimming. All sequences were calibrated using a known length on the animal in the dorsal view to avoid errors due to parallax. Actual swimming speed of the study animal was calculated by digitizing the start and end points of a stationary body landmark of the fish (such as the eye, rostrum, or base of the first dorsal fin ray) as it moved through the field of view. The distance between these two points over time was added to the rate of water flow against the direction of swimming to determine the fish's true swimming speed, which was then converted to body lengths per second (BL/sec) for each animal.

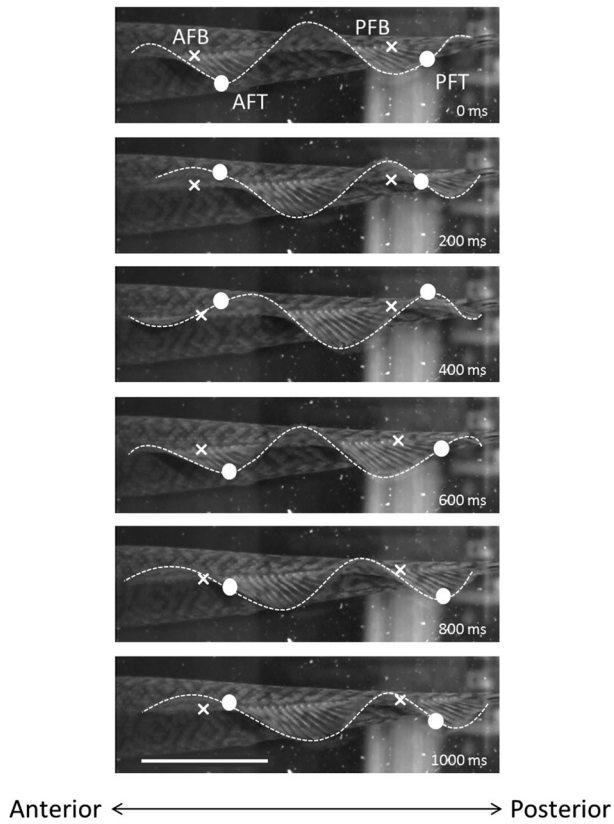

Figure 3. Time-lapse of ribbon-fin movement during steady swimming over one second. Waves traveling along the length of the fin are depicted at 200 ms intervals. The edge of the fin is traced with a dashed white line. Scale bar: 5 cm. Digitized points: AFB, anterior fin ray base; AFT, anterior fin ray tip; PFB, posterior fin ray base; PFT, posterior fin ray tip. Crosses indicate digitized landmarks for the base of the fin ray, and circles indicate digitized landmarks for the tip of the fin ray.

Four landmarks were manually digitized frame by frame (every 25 ms) from the dorsal view of the ribbon-fin throughout the swimming sequence: anterior fin ray base (AFB), anterior fin ray tip (AFT), posterior fin ray base (PFB), and posterior fin ray tip (PFT; Fig. 3). Anterior fin ray kinematics was consistently measured at the 10th anterior-most fin ray, and posterior fin ray kinematics was measured at the 10th posterior-most fin ray in all experimental individuals. Differences in the lengths of the two fin rays were measured and standardized accordingly to accurately compare their movement patterns.

Anterior and posterior lateral displacement of the fin ray tips relative to the fin ray bases were plotted against time to measure frequency and amplitude for describing the propulsive wave. To account for distortion of lateral displacements of the fin rays due to possible rolling of the fish, videos were only included in the analyses when the midline of the body was equidistant from the lateral sides of the body. A completed oscillation of the fin ray tip relative to the base represented the passing of one wave through the ribbon-fin. Using the plot of fin ray tip movements relative to its base over time (Fig. 4), frequency (f) was measured by determining the inverse of the period (T) for one wave ($f = 1/T$), and amplitude was calculated by determining the total distance in the y-axis from the peak of the wave to the trough of the wave in the plot and dividing by two. Because of the uncertainty of the ribbon-fin measurements obtained previously (Blake, '80, '83; Fei et al., 2005), frequency and amplitude were also measured directly from the video sequence of ribbon-fin undulations (as opposed to using a plot of fin ray oscillations over time), although no significant differences were found between the two methods (paired t-tests: $P < 0.05$). A third measurement, wavelength (λ), was also obtained to describe the propulsive wave by measuring the anterior–posterior distance between the peaks of two consecutive waves along the length of the fin. Finally, wave speed was determined using the equation:

$$\upsilon = \lambda f \quad (1)$$

where υ is wave speed, λ is wavelength, f is frequency. Frequency, amplitude, wavelength, and wave speed were measured for each wave in each video (i.e., four waves were measured in the graph of fin ray oscillations in Fig. 4). Means of the wave variables among waves from each video were used for analyses. Values for amplitude and wavelength were standardized by dividing these values by the length of the ribbon-fin (RFL) (Blake, '83). Wave speed was standardized using body length (BL) (Fei et al., 2005) to directly compare to swimming speed.

To analyze the kinematics of pectoral fin movements, we manually digitized six landmarks on the right pectoral fin: the tip

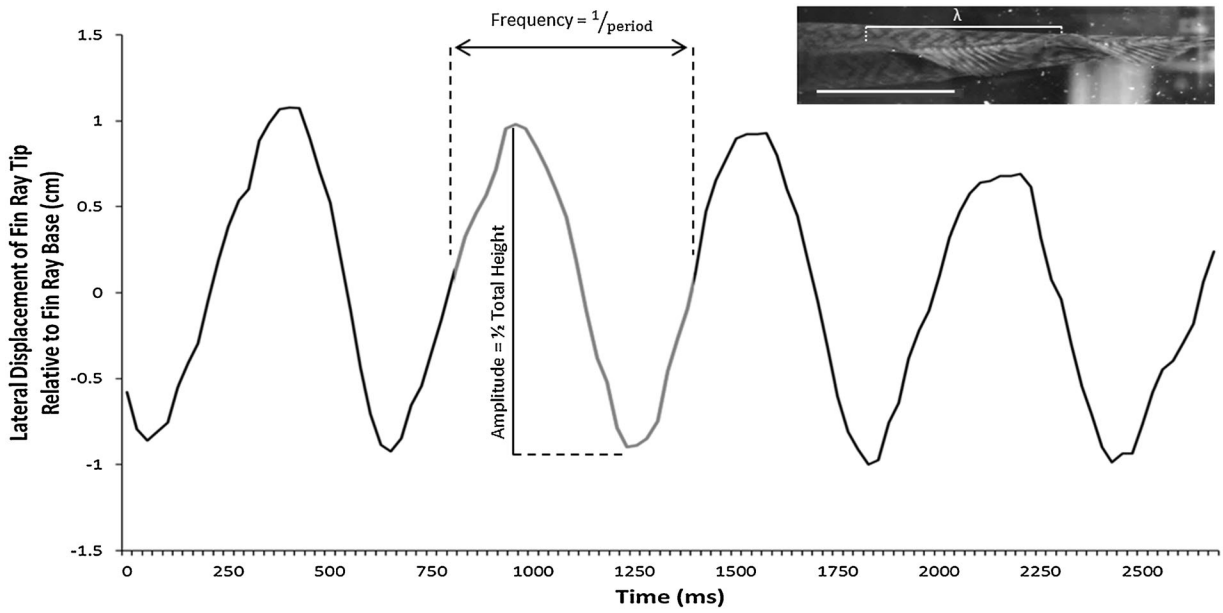

Figure 4. Graph of representative wave cycle at the anterior region of the ribbon-fin during forward propulsion in *Amia calva*. Lateral displacement of the 10th anterior-most fin ray tip is graphed relative to the fin ray base over time. Each complete oscillation of the fin ray represents the production of a single propulsive wave. Frequency (Hz) is measured using the inverse of the period (duration) of each wave. Amplitude is equal to half of the vertical distance between the peak and trough of the oscillation. Wavelength (λ) is the total horizontal distance between consecutive wave peaks.

of the leading fin ray (LT), base of the leading fin ray (LB), tip of the longest medial fin ray (MT), base of the longest medial fin ray (MB), tip of the trailing fin ray (TT), and base of the trailing fin ray (TB; Fig. 5). We digitized three fin rays along the length of the pectoral fin to account for the curvature of the pectoral fin throughout a fin beat. Movement of the tips of the fin rays relative to the body (measured at the base of the fin rays) were graphed against time to measure the frequency of the fin beats as the pectoral fins were used for propulsion. Each pectoral fin beat consisted of a single power stroke and its subsequent recovery stroke (Webb, '73). In addition, we measured the angles of each of the three fin rays relative to the long axis of the body when the fin was maximally adducted and abducted throughout the fin beat. The difference in these two angles was used as a measure of the amplitude of the fin beat for each of the three digitized fin rays.

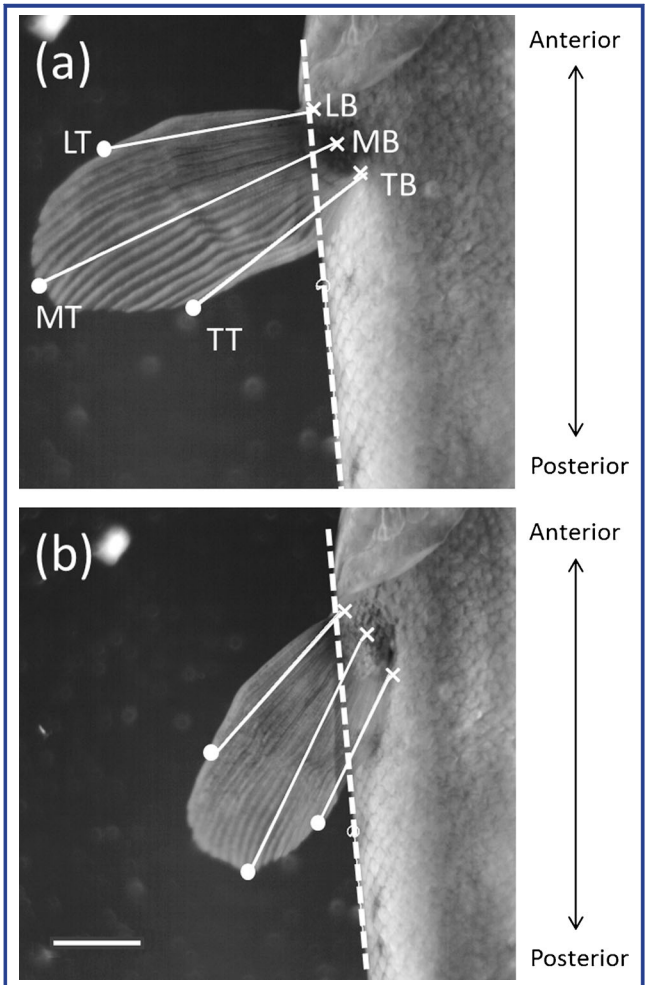

Figure 5. Pectoral fin at maximum (a) adduction and (b) abduction. Scale bar: 1 cm. Digitized points: LT, leading edge tip; LB, leading edge base; MT, median ray tip; MB, median ray base; TT, trailing edge tip; TB, trailing edge base. Crosses indicate digitized landmarks for the base of the fin ray, and circles indicated digitized landmarks for the tip of the fin ray. Changes in fin angle were measured using the orientation of the fin ray (solid bars) relative to the length of the body (dashed bars).

Statistical Analyses

To test if wave properties differ along the length of the fin (**Question 1**), paired *t*-tests were used to analyze differences in the four wave variables (frequency, amplitude, wavelength, and wave speed) between anterior and posterior regions of the ribbon-fin. Analyses compared the means of each wave variable over all swimming speeds recorded for each individual.

To determine how the ribbon-fin is used to control swimming speed (**Question 2**), a stepwise multiple regression was used to assess which of the four wave variables was the best predictor(s) of swimming speed. Multiple regressions were conducted using data from each individual separately, and with data from all individuals pooled together. Additionally, a Pearson correlation analysis tested for correlations among the four wave variables, and an analysis of covariance (ANCOVA) performed under the general linear model tested for consistency in the relationship between the variables and swimming speed across individuals.

To assess the influence of pectoral fin movements on ribbon-fin locomotion (**Question 3**), ribbon-fin kinematics data was collected when the ribbon-fin was used alone and when the ribbon-fin was used simultaneously with the pectoral fins. The relationships between the wave parameters and swimming speed under these two conditions were compared using an ANCOVA. Additionally, a multiple regression was also used to determine which of the two pectoral fin variables (frequency and change in angle) best predicted swimming speed in two individuals. All statistical analyses were performed using SYSTAT 13.0.

RESULTS

After correcting for actual swimming speed against controlled water flow in the flume, *Amia* were found to swim steadily using only the ribbon-fin at speeds of 0.12–0.73 BL/s. Ribbon-fin undulations produced symmetric sinusoidal waves along the fin, in which amplitude was equal in the positive and negative directions from the midline of the wave. Mean frequency, amplitude, wavelength, and wave speed of the propulsive waves over all swimming speeds are provided in Table 1.

Paired *t*-tests showed no significant differences in any of the wave parameters at anterior and posterior regions of the ribbon-fin during steady swimming in all of the experimental animals (Table 2, Fig. 6). Therefore, values for frequency, amplitude, wavelength, and wave speed measured at both ends of the ribbon-fin were averaged in subsequent analyses.

Pearson correlation analysis of the ribbon-fin wave parameters showed no significant relationships among frequency, amplitude, and wavelength, irrespective of pectoral fin use (Table 3).

Table 1. Summary of ribbon-fin kinematics at anterior and posterior regions of the fin.

	Frequency (Hz)		Amplitude (cm)		Wavelength (cm)		Wave speed (Bl/sec)	
	Anterior	Posterior	Anterior	Posterior	Anterior	Posterior	Anterior	Posterior
Ribbon-fin used without pectoral fins	2.42 ± 0.71	2.45 ± 0.72	0.91 ± 0.16 (*0.067*)	0.91 ± 0.17 (*0.067*)	6.61 ± 0.79 (*0.490*)	6.63 ± 0.85 (*0.491*)	16.05 ± 5.32 (*0.536*)	16.31 ± 5.42 (*0.544*)
Ribbon-fin used with pectoral fins	2.68 ± 0.68	2.72 ± 0.69	0.94 ± 0.18 (*0.067*)	0.94 ± 0.16 (*0.067*)	6.41 ± 0.92 (*0.462*)	6.51 ± 0.95 (*0.469*)	17.01 ± 4.28 (*0.555*)	17.51 ± 4.46 (*0.571*)

Values are raw means ± SEM.
Italicized values for Amplitude and Wavelength are means corrected for ribbon-fin length.
Italicized values for Wave Speed are means corrected for body length.

However, wave speed showed a significant relationship with both frequency and wavelength. We found no significant effects of individual on the changes in each of the wave parameters with swimming speed (Table 4). Multiple regressions demonstrated a significant positive relationship between wave frequency and swimming speed (Ind. 1–4: $R^2 = 0.60, 0.82, 0.57, 0.87$, respectively; $P < 0.05$) and between wave speed and swimming speed (Ind. 1–4: $R^2 = 0.49, 0.77, 0.67, 0.80$, respectively; $P < 0.05$) in all individuals, but no significant relationship between amplitude or wavelength with swimming speed (Table 5, Fig. 7).

Qualitative observations of pectoral fin movements during ribbon-fin swimming revealed that synchronous movements of the right and left pectoral fins could occur at any swimming speed. However, use of the pectoral fins simultaneously with the ribbon-fin was found to be unpredictable in all experimental animals, occurring at swimming speeds of 0.11–0.83 BL/sec. Multiple regression analyses of the changes in ribbon-fin wave parameters with swimming speed showed identical results when the pectoral fins were used simultaneously (Table 5). Swimming speed was again determined to be best predicted by ribbon-fin wave frequency (Ind. 1–4: $R^2 = 0.45, 0.64, 0.71, 0.58$, respectively; $P < 0.05$) and wave speed (Ind. 1–4: $R^2 = 0.38, 0.67, 0.55, 0.34$, respectively; $P < 0.05$), while no significant relationship was found in amplitude or wavelength with swimming speed (Fig. 8). Although the slopes of the regression lines of frequency and swimming speed when the pectoral fins were used versus not used did not differ significantly (ANCOVA: F-ratio = 2.500, $P = 0.117$), the height of the regression line was significantly greater when the pectoral fins were used ($P < 0.05$; Fig. 9). Statistical analysis of the pectoral fin kinematics detected no significant relationships between swimming speed and pectoral fin movements at any of the points digitized along the fin (Table 6, Fig. 10).

DISCUSSION

Do the Wave Properties of the Ribbon-Fin Undulations Change Along the Length of the Fin?

There is no significant difference in frequency, amplitude, wavelength, or wave speed between the anterior and posterior regions of the ribbon-fin in *Amia* (Fig. 6). Because less than two waves were observed traveling along the fin at all swimming speeds, it was not necessary to measure the wave parameters at more than two points in order to determine if there are any differences along the length of the fin. Although no differences were found along the ribbon-fin in *Amia*, it cannot be assumed to be the case in all ribbon-fin swimmers because the ribbon-fin of *Amia* is shorter in length than most other species. Compared to most knifefishes, for example, the bowfin has a shorter ribbon-fin relative to total body length, which ends at the caudal peduncle just before a distinct caudal fin. The fin rays of the bowfin ribbon-fin are the same length along the fin, thus generating symmetrical waves for propulsion. Most knifefish (including members of Osteoglossiformes and Gymnotiformes) have a longer ribbon-fin that runs almost the entire length of the body, and usually tapers

Table 2. Summary of paired t-tests comparing wave parameters at anterior and posterior ends of the ribbon-fin.

	Frequency			Amplitude			Wavelength			Wave speed		
Ind.	t-Stat	d.f.	P-value	t-Stat	d.f.	P-value	t-Stat	d.f.	P-value	t-Stat	d.f.	P-value
1	−0.214	10	0.835	−1.473	10	0.172	−1.669	10	0.126	−0.776	10	0.456
2	−0.202	14	0.843	−0.233	14	0.819	1.319	14	0.208	0.828	14	0.422
3	−0.674	15	0.510	−0.914	15	0.375	−0.346	15	0.734	−0.617	15	0.547
4	−1.782	10	0.105	1.585	10	0.144	0.236	10	0.818	−1.693	10	0.121

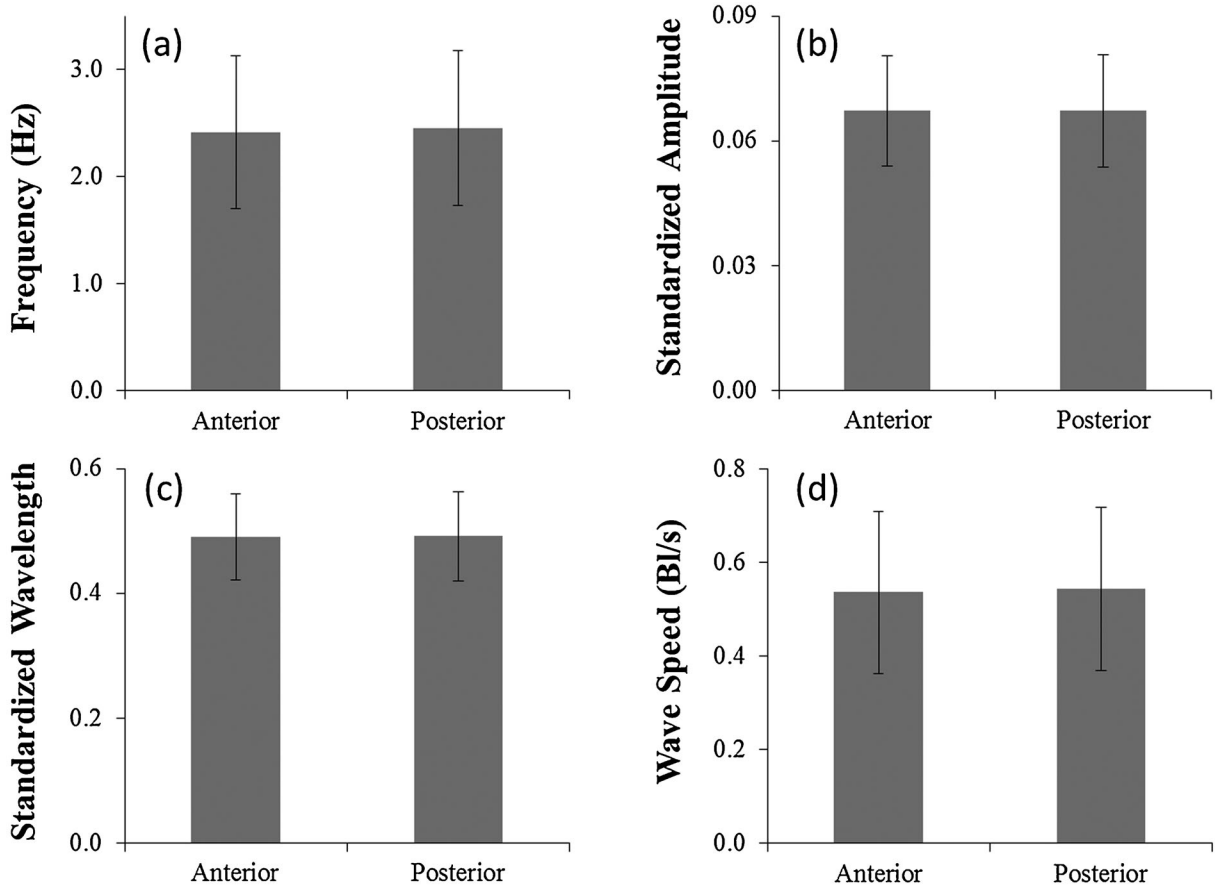

Figure 6. Mean values of (a) frequency, (b) amplitude, (c) wavelength, and (d) wave speed of propulsive waves produced by the ribbon-fin over all recorded swimming speeds in *Amia calva* using data from all individuals pooled together (n = 4). Values are provided at anterior and posterior regions of the ribbon-fin. Amplitude and wavelength are standardized for ribbon-fin length.

off at the posterior end of the fish, rather than having a distinct propulsive caudal fin. This disparity in ribbon-fin length may result in significant differences in the propulsive waves generated at various regions of the ribbon-fin in knifefish. Fei et al. (2005) suggested that wave amplitude decreases posteriorly in the African aba aba (*Gymnarchus niloticus*), which exhibits a tapered dorsal ribbon-fin in which the length of the fin rays decreases posteriorly, although this was not empirically demonstrated.

Table 3. Pearson correlation analysis of ribbon-fin wave parameters.

	Used without pectoral fins		Used with pectoral fins	
Ribbon-fin wave parameters	PCC	*P*-value	PCC	*P*-value
Frequency-amplitude	0.322	0.209	0.504	0.114
Frequency-wavelength	0.013	0.962	0.223	0.511
Frequency-wave speed	0.861	**0.000**	0.750	**0.008**
Amplitude-wavelength	−0.188	0.485	0.012	0.971
Amplitude-wave speed	0.189	0.484	0.414	0.206
Wavelength-wave speed	0.516	**0.041**	0.715	**0.013**

PCC, Pearson correlation coefficient.
Significant values ($P < 0.05$) are highlighted in bold.

Table 4. Results from analysis of covariance for individual effects on changes in wave parameters with swimming speed.

	Used without pectoral fins			Used with pectoral fins		
Ribbon-fin wave parameter	*F*-ratio	d.f.	*P*-value	*F*-ratio	d.f.	*P*-value
Frequency	0.432	3	0.731	0.028	3	0.993
Standardized amplitude	0.412	3	0.745	2.334	3	0.088
Standardized wavelength	0.569	3	0.638	1.174	3	0.332
standardized wave speed	0.187	3	0.904	0.283	3	0.837

Therefore, it is not possible to conclude that the results observed in *Amia* are consistent among all other ribbon-fin swimmers without quantitative data from other species.

How is the Ribbon-Fin Used to Control Swimming Speed?

When swimming at slower speeds (below 1 BL/sec), bowfin swam steadily with the ribbon-fin while the body and caudal fin remained rigid. Therefore, in order to increase or decrease swimming speed within the range of speeds analyzed, individuals must rely on changing the patterns of one or more ribbon-fin wave parameters. Two general methods by which the ribbon-fin can be predicted to increase swimming speed are (a) increasing wave amplitude and wavelength to produce larger waves with greater propulsive force per wave, or (b) increasing wave frequency to produce more propulsive waves over time (Blake, '83). Increasing all three wave parameters to generate faster, larger waves is also possible, but would be energetically costly during steady swimming. Kinematic analysis of the ribbon-fin revealed wave frequency to be the most reliable predictor of swimming speed in all four individuals, while amplitude and wavelength show no significant relationship with swimming speed (Fig. 7). Furthermore, values for amplitude and wavelength are highly variable with swimming speeds (Fig. 7b and c; Fig. 8b and c) suggesting less control of these two variables during ribbon-fin swimming by *Amia*. Instead, *Amia* relies on increasing the frequency of the waves to increase swimming speed. Because frequency increases with swimming speed and wavelength does not change, the significant positive relationship between wave speed and swimming speed is expected (Table 5).

Wave frequency was also found to significantly increase with swimming speed in the black ghost knifefish (*Apteronotus albifrons*) at slow speeds below one body length per second (Ruiz-Torres et al., 2012). At greater speeds, however, frequency remained constant while increasing wave amplitude became more prominent. A gait transition is also observed at the same relative

Table 5. Results from regression analysis of changes in wave parameters with swimming speed.

		Used without pectoral fins			Used with pectoral fins		
Ribbon-fin wave parameter	Individual	Regression equation	R^2	*P*-value	Regression equation	R^2	*P*-value
Frequency	1	$y=2.90x+1.51$	0.60	**0.005**	$y=2.29x+2.05$	0.45	**0.005**
	2	$y=2.99x+1.48$	0.82	**0.000**	$y=2.53x+1.94$	0.64	**0.002**
	3	$y=2.60x+1.63$	0.57	**0.001**	$y=2.45x+1.99$	0.71	**0.001**
	4	$y=3.52x+1.27$	0.87	**0.000**	$y=2.37x+2.01$	0.58	**0.017**
Standardized amplitude	1	$y=0.01x+0.06$	0.01	0.790	$y=-0.02x+0.07$	0.07	0.307
	2	$y=0.02x+0.05$	0.25	0.057	$y=0.03x+0.05$	0.33	0.062
	3	$y=0.01x+0.06$	0.10	0.241	$y=0.02x+0.06$	0.29	0.090
	4	$y=0.01x+0.06$	0.32	0.069	$y=0.01x+0.06$	0.05	0.567
Standardized wavelength	1	$y=0.05x+0.43$	0.06	0.456	$y=-0.13x+0.50$	0.14	0.150
	2	$y=-0.01x+0.45$	0.01	0.863	$y=-0.01x+0.45$	0.01	0.883
	3	$y=0.10x+0.41$	0.10	0.221	$y=0.11x+0.39$	0.18	0.197
	4	$y=0.05x+0.43$	0.07	0.417	$y=-0.06x+0.47$	0.04	0.600
Wave speed	1	$y=0.75x+0.26$	0.49	**0.016**	$y=0.39x+0.45$	0.38	**0.012**
	2	$y=0.70x+0.28$	0.77	**0.000**	$y=0.54x+0.38$	0.67	**0.001**
	3	$y=0.65x+0.30$	0.67	**0.000**	$y=0.51x+0.39$	0.55	**0.009**
	4	$y=0.80x+0.24$	0.80	**0.000**	$y=0.39x+0.45$	0.34	**0.048**

Significant values ($P<0.05$) are highlighted in bold.

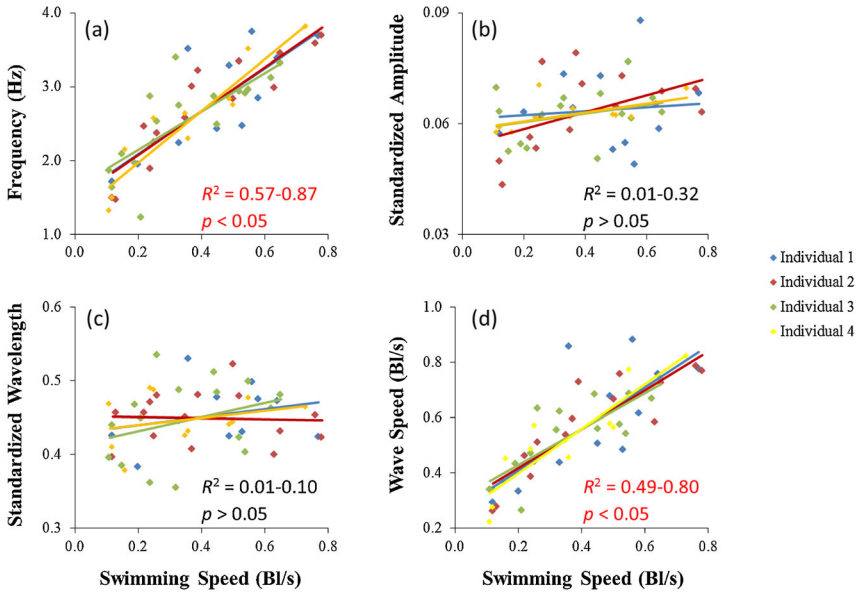

Figure 7. Relationships between ribbon-fin wave (a) frequency, (b) amplitude, (c) wavelength, and (d) wave speed with swimming speed in *Amia calva* when pectoral fins are not used. Amplitude and wavelength are standardized for ribbon-fin length. Mean values for each wave parameter is plotted against swimming speed for each individual (n = 4), which are depicted in different colors. Statistical significance and the range of R^2 values among individuals are provided for each wave parameter measured. Regression equations are provided in Table 5.

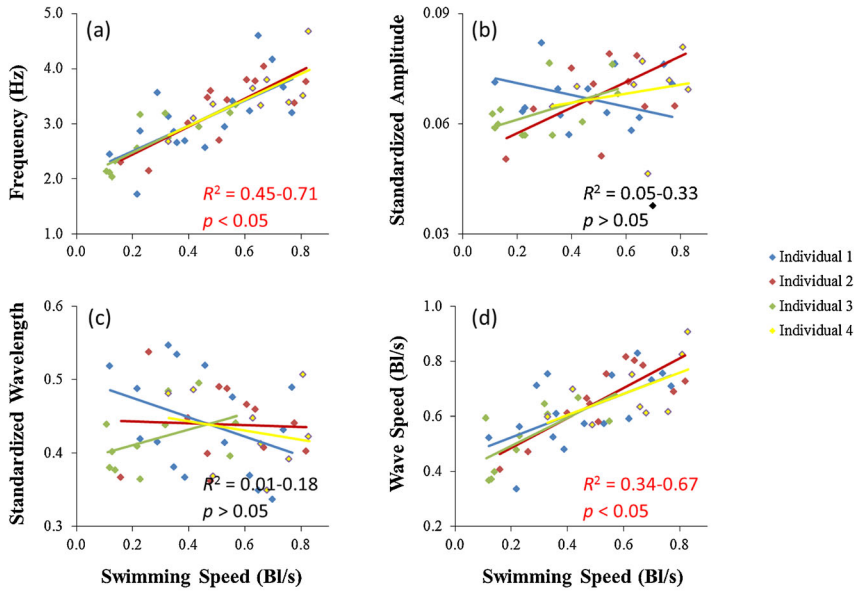

Figure 8. Relationships between ribbon-fin wave (a) frequency, (b) amplitude, (c) wavelength, and (d) wave speed with swimming speed in *Amia calva* when *pectoral fins are used simultaneously.* Amplitude and wavelength are standardized for ribbon-fin length. Mean values for each wave parameter is plotted against swimming speed for each individual (n = 4), which are depicted in different colors. Statistical significance and the range of R^2 values among individuals are provided for each wave parameter measured. Regression equations are provided in Table 5.

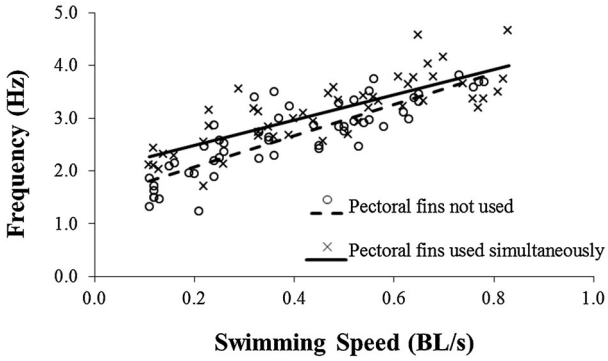

Figure 9. Relationships between ribbon-fin wave frequency with swimming speed in *Amia calva* when ribbon-fin is used with and without pectoral fins. Mean frequency is plotted against swimming speed using data from all individuals pooled together. Regression equations: pectoral fins not used, $y = 2.98x + 1.48$, $R^2 = 0.72$, $P < 0.05$; pectoral fins used simultaneously, $y = 2.39x + 2.00$, $R^2 = 0.64$, $P < 0.05$.

speed (~1 BL/sec) in the bowfin, except that the transition here is one from increasing ribbon-fin wave frequency at slow speeds, to increasing movement of the body and caudal fin at higher speeds. The results of these studies suggest that modulating wave frequency may be effective at slow speeds, but does not generate enough propulsion for faster swimming. However, this method of regulating swimming speed is not observed in the African aba aba (*Gymnarchus niloticus*), which demonstrates a significant increase in amplitude, wavelength, and wave speed with swimming speed, and an inverse relationship with frequency (Fig. 11) (Fei et al., 2005). Although Fei et al. (2005) used a slightly different experimental design (the fish was observed swimming in stationary water, rather than using a controlled flume), the data demonstrate a noteworthy difference in control of a dorsal ribbon-fin in two phylogenetically distant species. Contrary to the bowfin, the African aba aba utilizes waves of greater amplitude and length to generate more force per wave for propulsion with increasing swimming speed.

Data on ribbon-fin swimming in other distantly related species also suggest notable differences and control of the fin for propulsion (Table 7). While these studies did not analyze changes in ribbon-fin movement with swimming speed, overall means of ribbon-fin kinematics across species are highly variable. For example, the use of a ventral ribbon-fin by gymnotids and the African brown knifefish show greater wave frequencies than the dorsal ribbon-fin swimmers (excluding the seahorse), and have been observed swimming at relatively greater speeds (Blake, '83). This suggests a difference in the mechanism of dorsal versus ventral ribbon-fin locomotion.

This variability in ribbon-fin use may relate to ecological differences among species. For example, many ribbon-fin

Table 6. Results from regression analysis of changes in pectoral fin movement parameters with swimming speed.

Pectoral fin movement parameter	Individual	Leading edge			Medial ray			Trailing edge		
		Regression equation	R^2	*P*-value	Regression equation	R^2	*P*-value	Regression equation	R^2	*P*-value
Frequency	1	$y = 0.34x + 0.43$	0.13	0.159	$y = 0.33x + 0.44$	0.14	0.477	$y = 0.43x + 0.40$	0.20	0.119
	2	$y = 0.52x + 0.23$	0.48	0.311	$y = 0.55x + 0.22$	0.50	0.503	$y = 0.58x + 0.21$	0.49	0.929
Change in angle	1	$y = -24.16x + 37.86$	0.34	0.281	$y = -9.29x + 31.71$	0.12	0.477	$y = -11.94x + 25.59$	0.19	0.924
	2	$y = -10.96x + 47.41$	0.07	0.646	$y = -20.01x + 50.23$	0.26	0.278	$y = -15.72x + 35.29$	0.16	0.393

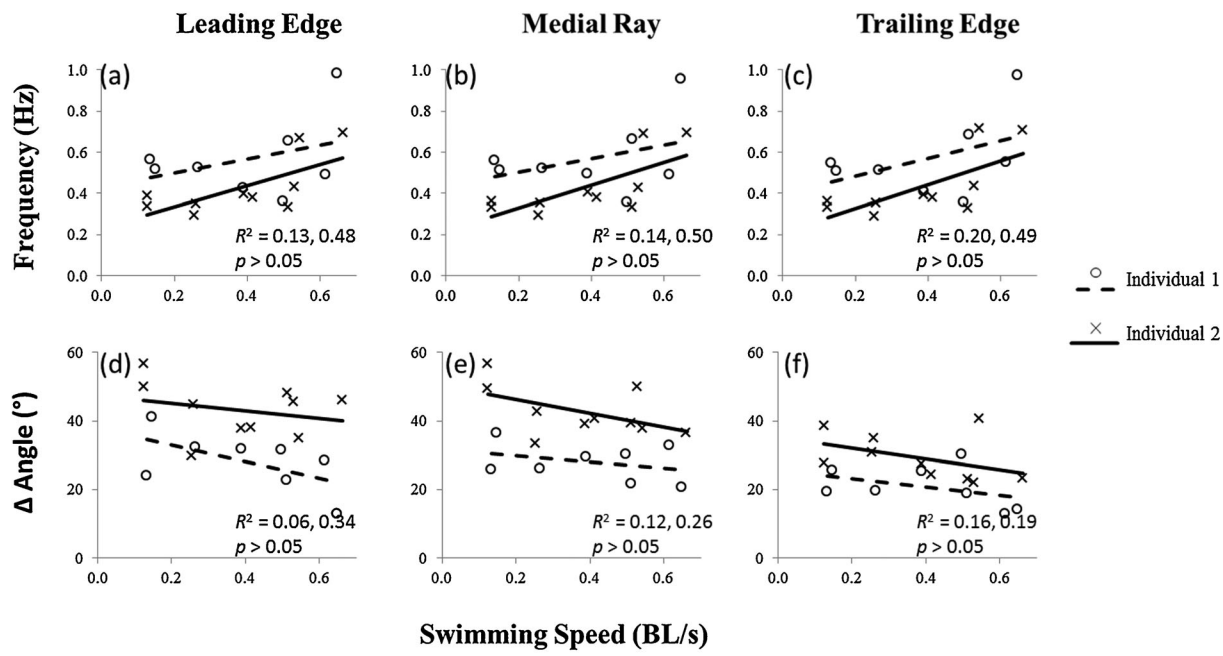

Figure 10. Relationships between pectoral fin (**a–c**) frequency and (**d–f**) change in angle with swimming speed in *Amia calva*, measured at the leading edge, medial ray, and trailing edge of the right pectoral fin. Mean values for each movement parameter is plotted against swimming speed for each individual (n = 2). Statistical significance and the range of R^2 values for each experimental individual are provided for each movement parameter measured at each point on the fin. Regression equations are provided in Table 6.

swimmers produce a weak electric field in the water column around their bodies and use electric sensing for navigation and predation (Lissmann, '51; Lissmann and Machin, '58). In addition to increasing maneuverability and energetic efficiency, several studies propose that ribbon-fin locomotion may have specifically evolved in electric fishes because the fin provides propulsion without use of the trunk musculature, thus allowing for greater control of the electroreceptor organs throughout the body (Lissmann and Machin, '58; Blake, '83; Lannoo and Lannoo, '93; ; Nelson and MacIver, '99). By holding the body rigid while using the ribbon-fin, weakly electric fish such as the African aba aba and the black ghost knifefish maximize sensory reception for maneuvering and predation. There is no evidence to date that bowfin use electroreception.

Additionally, differences in ribbon-fin kinematics may be linked with morphological differences across species. While the bowfin ribbon-fin is composed of fairly equal length fin rays, knifefish and the African aba aba possess a longer ribbon-fin that tapers off at the posterior end. Therefore, differences in each wave parameter may be related to differences in the length of the ribbon-fin and/or the length of the fin rays along the length of the fin between the two species (i.e., longer fin rays would likely generate waves of greater amplitude).

Is the Ribbon-Fin the Primary Propulsor at Slow Swimming Speeds?

This study is the first to address the simultaneous use of other fins for propulsion during ribbon-fin swimming. When moving in a rowing manner during ribbon-fin swimming, the pectoral fins were predicted to provide additional propulsive forces during slow steady swimming in *Amia*. However, analyses of ribbon-fin use with and without pectoral fin influences demonstrated no difference in the ribbon-fin wave parameters controlling swimming speed (i.e., wave frequency was still the best predictor of swimming speed; Figs. 7 and 8). Thus, ribbon-fin control of speed is identical, regardless of pectoral fin movements. Additionally, the pectoral fin movements were found to have no significant influence on swimming speed (Fig. 10), suggesting that the pectoral fins are in fact not contributing to propulsion. Pectoral fin movements may indeed hinder propulsion, mitigated by the observed increased wave frequency of the ribbon-fin at a given speed (Fig. 9).

We hypothesize that pectoral fin movements serve a secondary role that is not associated with propulsion during ribbon-fin locomotion. While video sequences in which the fish was turning (and thus not swimming steadily) were omitted from analyses, it is plausible that the pectoral fins make slight undetectable maneuvers and adjustments in the water column, or produce

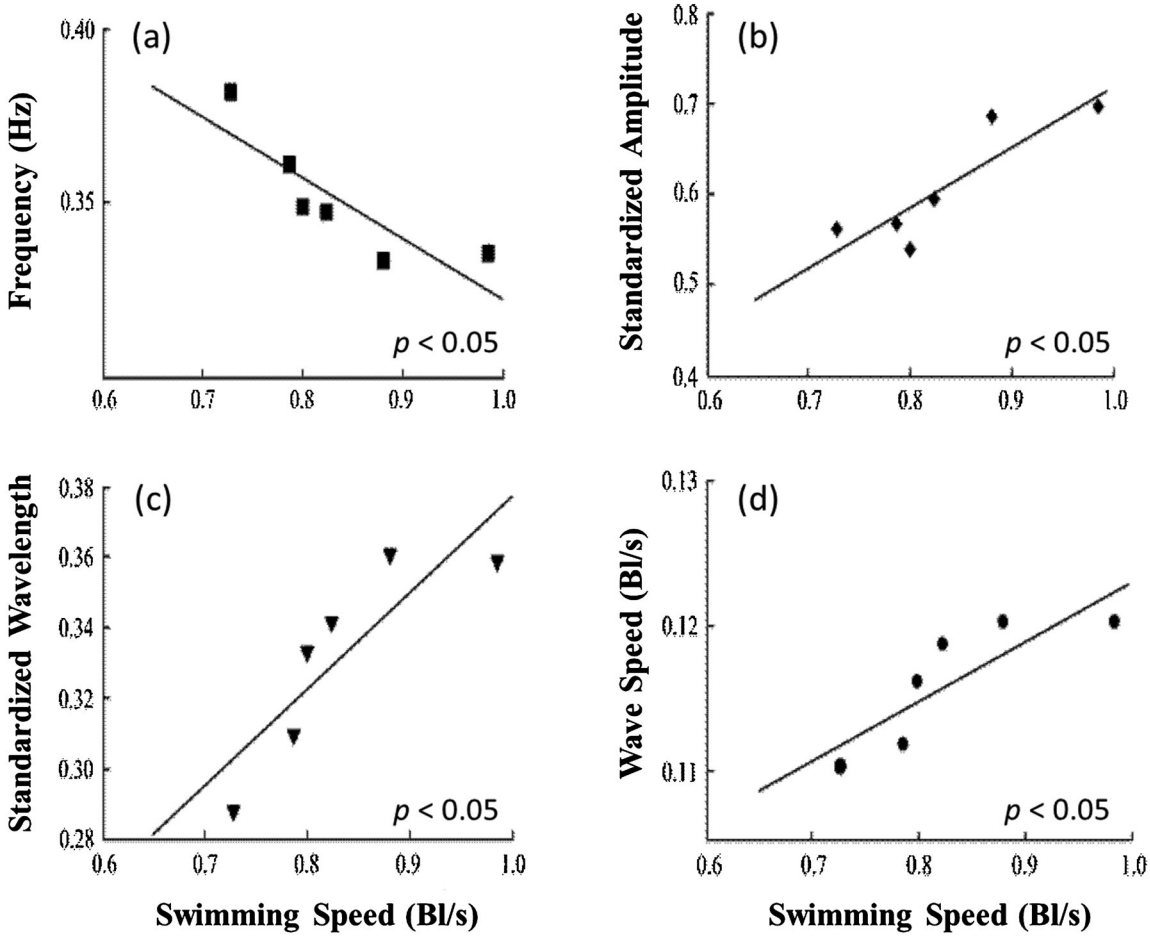

Figure 11. Relationships between ribbon-fin wave (a) frequency, (b) amplitude, (c) wavelength, and (d) wave speed with swimming speed in *Gymnarchus niloticus* (n = 1). Amplitude and wavelength are standardized for body length. All regressions show statistically significant relationships (adapted from Fei et al., 2005).

Table 7. Summary of ribbon-fin kinematics across species.

Species	Ribbon-fin orientation	Swimming speed (BL/sec)[a]	Mean frequency (Hz)	Mean amplitude[b]	Mean wavelength[b]	Source
Bowfin (*Amia calva*)	Dorsal	1	2.4	0.07	0.49	This study
African aba aba (*Gymnarchusniloticus*)	Dorsal	1	2.4	0.08	0.51	Blake ('80)
Seahorse (*Hippocampus hudsonius)*	Dorsal	1.2	41	0.30	0.29	Blake ('80)
Gymnotids	Ventral	5.0	2–15	0.05	0.4	Blake ('83)
African brown knifefish (*Xenomystus nigri*)	Ventral	5.0	2–15	0.10	0.6	Blake ('83)

Range is provided where means were not listed.
[a]Values are maximum swimming speeds recorded.
[b]Standardized for ribbon-fin length.

forces associated with lift (Webb, '73; Drucker and Lauder, 2001). Analyses of the hydrodynamics associated with pectoral fin movements in *Amia* are necessary to accurately ascertain the purpose of pectoral fin oscillations during ribbon-fin swimming. Although the results of this study do not suggest that the pectoral fins influence ribbon-fin propulsion in *Amia*, the simultaneous use of other fins during ribbon-fin swimming should not be ignored in future studies on other species with similar swimming modes.

Ecological and Evolutionary Implications

Utilizing ribbon-fin locomotion has been suggested to allow for greater maneuverability and energetic efficiency when traveling at slow swimming speeds in various ribbon-fin swimmers (Blake, '83; Blake, 2004), and can be hypothesized to provide a similar benefit in *Amia*. This is the primary propulsive system that the fish employs when searching for prey, navigating through complex environments, and station-holding while in slow moving waters. The ribbon-fin provides the animal with a means of maintaining position without expending a large amount of energy. Another unique benefit of this body form is the ability to swim backwards with remarkable ease by simply reversing the direction of the wave undulations (Lannoo and Lannoo, '93; Shirgaonkar et al., 2008). Several other fish use this swimming mode in similar environments, indicating that ribbon-fin swimming may be an adaptation in slow-moving waters or environments with complex architectures.

The ribbon-fin also provides steady swimming while keeping the body rigid, an adaptation that is suggested to be critical in effectively generating weak electric fields and sensing predators and prey items in weakly electric fish (Nelson and MacIver, '99; MacIver et al., 2010). A common debate occurs in interpreting the evolution of the ribbon-fin as an adaptation for electroreception, energetically efficient swimming, or increased maneuverability for foraging in complex environments (Lissmann and Machin, '58; Blake, '83; Lannoo and Lannoo, '93). While weakly electric fish certainly benefit from using ribbon-fin locomotion to enhance electroreception, several species (e.g., ghost knifefish) also utilize the enhanced maneuverability for navigating through small enclosures and complex environments with both forward and backward swimming.

The ribbon-fin, therefore, provides a definitive example of a convergently evolved trait in fishes. Expressed in several groups of distantly related animals, the ribbon-fin is not found in a single common ancestor of ribbon-fin swimmers. Instead, the elongation of the dorsal or anal fin to produce undulatory waves has occurred in many groups due to various selective pressures which may include the need for a rigid body during steady swimming, decreased energy expenditure, and/or greater maneuverability. Although less common than more typical forms of swimming (i.e., various forms of BCF propulsion), the ribbon-fin has evolved in multiple groups of ray-finned fishes. Ribbon-fin swimming may in fact be a basal mode of fish locomotion because it is found in several extant primitive fish including *Amia calva* and *Protanguilla palau*, a newly discovered species of that is suggested to represent one of the most basal lineages of true eels (Johnson et al., 2012).

Biomimetics

One of the primary applications of studies based on aquatic and terrestrial locomotion is the development of biologically-inspired designs as a means of solving problems in engineering and mechanics using the solutions that evolution has already provided. These designs have become the basis of constructing robots and devices with high mechanical efficiency, such as robotic autonomous underwater vehicles (AUVs). The evolutionary designs of fish fins are commonly exploited in such artificial systems (Sfakiotakis et al., '99; Blake, 2004), and are in great demand for advancing scientific research and exploration.

Because the ribbon-fin is used for both forward and backwards swimming with minimal body movement and high energetic efficiency, this design is of high interest in the development of robotic AUVs. The evolutionary design of the ribbon-fin has already been mimicked in the development of *RoboGnilos*, based on the dorsal ribbon-fin of *Gymnarchus niloticus* (Hu et al., 2009; Zhou et al., 2010) and *GhostBot*, based on the ventral ribbon-fin of *Apteronotus albifrons* (MacIver et al., 2004; Epstein et al., 2006; Curet et al., 2011). While these studies have used the robotic models to describe thrust production and efficiency of undulatory wave propulsion, increasing our understanding of the kinematics, hydrodynamics, and mechanical properties of ribbon-fin swimming in live animals might provide important clues that underlie the versatility or efficiency of such systems. These studies would thus contribute to further development and improvements of these robotic systems and lead to more accurate next generation AUVs.

CONCLUSIONS

Kinematic analysis of the dorsal ribbon-fin in *Amia calva* demonstrates no differences in propulsive waves along the length of the fin, a significant relationship between frequency and wave speed with swimming speed, and no significant contribution of the pectoral fins in generating propulsion during ribbon-fin swimming. This baseline study provides a clear approach to quantifying the kinematics of propulsive undulatory waves that can be used to obtain comparative data from other ribbon-fin swimmers. Future studies should focus on comparing the use of a dorsal ribbon-fin to that of a ventral ribbon-fin across distant taxa. Analyses of the morphology, mechanical properties, and hydrodynamics of the ribbon-fin are also essential in understanding the efficiency of this system. A thorough comparative analysis of locomotion in ribbon-fin swimmers will provide greater insight into the convergent evolution of this swimming mode and may also lead to future advances in biomimetic designs.

ACKNOWLEDGMENTS

The authors would like to thank N. Radecker for her commitment as the primary caretaker of all of the animals in our labs. Undergraduate members of the Hofstra University Functional Morphology Lab (N. Blanchette and A. Cox), as well lab volunteers (Z.H.C. Liu) provided assistance in filming and digitizing video sequences. Thesis committee members and anonymous reviewers contributed significant input and constructive criticisms. Colleagues S. Gerry and A. Ward also afforded valuable advice concerning the experimental design and analysis associated with the work. We are also grateful to W. Stewart for assistance with illustrations.

LITERATURE CITED

Blake RW. 1976. Seahorse locomotion. J Mar Biol Assoc UK 56:939–949.

Blake RW. 1980. Undulatory median fin propulsion of two teleosts with different modes of life. Can J Zool 58:2116–2119.

Blake RW. 1983. Swimming in the electric eels and knifefishes. Can J Zool 61:1432–1441.

Blake RW. 2004. Fish functional design and swimming performance. J Fish Biol 65:1193–1222.

Breder CM. 1926. The locomotion of fishes. Zoologica 4:159–297.

Carlson RL, Lauder GV. 2011. Escaping the flow: boundary layer use by the darter *Etheostoma tetrazonum* (percidae) during benthic station holding. J Exp Biol 214:1181–1193.

Curet OM, Patankar NA, Lauder GV, MacIver MA. 2011. Aquatic manoeuvering with counter-propagating waves: a novel locomotive strategy. J R Soc Interface 8:1041–1050.

Drucker EG, Lauder GV. 2001. Wake dynamics and fluid forces of turning maneuvers in sunfish. J Exp Biol 204:431–442.

Epstein M, Colgate JE, MacIver MA. 2006. Generating thrust with a biologically-inspired robotic ribbon fin. In: Proceedings of the IEEE/RSJ international conference on intelligent robots systems (IROS), Beijing, China. p 2412–2417.

Fei L, Tian-jiang H, Guang-ming W, Lin-cheng S. 2005. Locomotion of *Gymnarchus niloticus*: experiment and kinematics. J Bionics Eng 2:115–121.

Grande L, Bemis WE. 1998. A comprehensive phylogenetic study of amiid fishes (Amiidae) based on comparative skeletal anatomy. An empirical search for interconnected patterns of natural history. J Vertebr Paleontol 18:1–690.

Hu TJ, Shen LC, Lin LX, Xu HJ. 2009. Biological inspirations, kinematics modeling, mechanism design and experiments on an undulating robotic fin inspired by *Gymnarchus niloticus*. Mech Mach Theory 44:633–645.

Hurley IA, Mueller RL, Dunn KA, Schmidt EJ, Friedman M, Ho RK, Prince VE, Yang Z, Thomas MG, Coates MI. 2007. A new time-scale for ray-finned fish evolution. Proc R Soc B 274:489–498.

Johnson GD, Ida H, Sakaue J, Sado T, Asahida T, Miya M. 2012. A 'living fossil' eel (Anguilliformes: protanguillidae, fam. Nov.) from an undersea cave in palau. Proc R Soc B 279:934–943.

Lannoo MJ, Lannoo SJ. 1993. Why do electric fishes swim backwards? An hypothesis based on gymnotiform foraging behavior interpreted through sensory constraints. Environ Biol Fish 36:157–165.

Lindsey CC. 1978. Form, function, and locomotory habits in fish. In: Hoar WS, Randall DJ, editors. Fish physiology. New York, NY: Academic Press. p 1–100.

Lissmann HW. 1951. Continuous electircal signals from the tail of a fish, *Gymnarchus niloticus* cuv. Nature 167:201–202.

Lissmann HW, Machin KE. 1958. The mechanism of object location in *Gymnarchus niloticus* and similar fish. J Exp Biol 35:451–486.

MacIver MA, Fontaine E, Burdick JW. 2004. Designing future underwater vehicles: principles and mechanisms of the weakly electric fish. Ieee J Oceanic Eng 29:651–659.

MacIver MA, Patankar NA, Shirgaonkar AA. 2010. Energy-information trade-offs between movement and sensing. Plos Comput Biol 6: e1000769.

Near TJ, Eytan RI, Dornburg A, Kuhn KL, Moore JA, Davis MP, Wainwright PC, Friedman M, Smith WL. 2012. Resolution of ray-finned fish phylogeny and timing of diversification. Proc Natl Acad Sci USA 109:13698–13703.

Nelson ME, MacIver MA. 1999. Prey capture in the weakly electric fish *Apteronotus albifrons*: sensory acquisition strategies and electrosensory consequences. J Exp Biol 202:1195–1203.

Ruiz-Torres R, Curet OM, Lauder GV, MacIver MA. 2012. Kinematics of the ribbon fin in hovering and swimming of the electric ghost knifefish. J Exp Biol 216:823–834.

Sfakiotakis M, Lane DM, Davies JBC. 1999. Review of fish swimming modes for aquatic locomotion. IEEE J Oceanic Eng 24:237–252.

Shirgaonkar AA, Curet OM, Patankar NA, MacIver MA. 2008. The hydrodynamics of ribbon-fin propulsion during impulsive motion. J Exp Biol 211:3490–3503.

Tytell ED, Lauder GV. 2004. The hydrodynamics of eel swimming: I. Wake structure. J Exp Biol 207:1825–1841.

Webb PW. 1973. Kinematics of pectoral fin propulsion in *Cymatogaster aggregata*. J Exp Biol 59:697–710.

Webb PW, Blake RW. 1985. Swimming. In: Hildebrand M, Bramble DM, Liem KF, Wake DB, editors. Functional vertebrate morphology. Cambridge, MA: Belknap Press Harvard. p 111–128.

Zhou H, Hu TJ, Xie HB, Zhang DB, Shen LC. 2010. Computational hydrodynamics and statistical modeling on biologically inspired undulating robotic fins: a two-dimensional study. J Bionic Eng 7:66–76.